






## Article

# Assessing Vulnerability to Cyclone Hazards in the World's Largest Mangrove Forest, The Sundarbans: A Geospatial Analysis

Mohammed<sup>1,2</sup>, Fahmida Sultana<sup>1,3</sup>, Ariful Khan<sup>1</sup>, Sohag Ahammed<sup>4</sup>, Md. Shamim Reza Saimun<sup>1</sup>, Md Saifuzzaman Bhuiyan<sup>1</sup>, Sanjeev K. Srivastava<sup>5</sup>, Sharif A. Mukul<sup>5,6,7,\*</sup> and Mohammed A. S. Arfin-Khan<sup>1,\*</sup>

<sup>1</sup> Department of Forestry and Environmental Science, School of Agriculture and Mineral Sciences, Shahjalal University of Science and Technology, Sylhet 3114, Bangladesh; md007@student.sust.edu (M.); fahmida-fes@sust.edu (F.S.); md.arifk65@student.sust.edu (A.K.); saimun-fes@sust.edu (M.S.R.S.); bhuiyan09-fes@sust.edu (M.S.B.)

<sup>2</sup> Department of Geography and Planning, University of Saskatchewan Saskatoon, Saskatoon, SK S7N 5C8, Canada

<sup>3</sup> School of Biosciences, Geography and Physics, Faculty of Science and Engineering, Swansea University, Singleton Park Swansea, Swansea SA2 8PP, UK

<sup>4</sup> Department of Forest Policy and Management, Faculty of Forestry and Environment, Bangabandhu Sheikh Mujibur Rahman Agricultural University, Gazipur 1706, Bangladesh; jafar36@student.sust.edu

<sup>5</sup> School of Science Technology and Engineering (SSTE), University of the Sunshine Coast, Maroochydore, DC QLD 4556, Australia; ssvivast@usc.edu.au

<sup>6</sup> Department of Environment and Development Studies, United International University, Dhaka 1212, Bangladesh

<sup>7</sup> Department of Earth and Environment, Florida International University, Miami, FL 33199, USA

\* Correspondence: smukul@usc.edu.au (S.A.M.); khan-for@sust.edu (M.A.S.A.-K.)



**Citation:** Mohammed, F.; Sultana, F.; Khan, A.; Ahammed, S.; Saimun, M.S.R.; Bhuiyan, M.S.; Srivastava, S.K.; Mukul, S.A.; Arfin-Khan, M.A.S. Assessing Vulnerability to Cyclone Hazards in the World's Largest Mangrove Forest, The Sundarbans: A Geospatial Analysis. *Forests* **2024**, *15*, 1722. <https://doi.org/10.3390/f15101722>

Academic Editors: Faridah Hanum Ibrahim, Abdul Latiff Mohamad and Waseem Razaq Khan

Received: 3 September 2024

Revised: 25 September 2024

Accepted: 27 September 2024

Published: 29 September 2024



**Copyright:** © 2024 by the authors. Licensee MDPI, Basel, Switzerland. This article is an open access article distributed under the terms and conditions of the Creative Commons Attribution (CC BY) license (<https://creativecommons.org/licenses/by/4.0/>).

**Abstract:** The Sundarbans is the world's largest contiguous mangrove forest with an area of about 10,000 square kilometers and shared between Bangladesh and India. This world-renowned mangrove forest, located on the lower Ganges floodplain and facing the Bay of Bengal, has long served as a crucial barrier, shielding southern coastal Bangladesh from cyclone hazards. However, the Sundarbans mangrove ecosystem is now increasingly threatened by climate-induced hazards, particularly tropical cyclones originating from the Indian Ocean. To assess the cyclone vulnerability of this unique ecosystem, using geospatial techniques, we analyzed the damage caused by past cyclones and the subsequent recovery across three salinity zones, i.e., Oligohaline, Mesohaline, and Polyhaline. Our study also examined the relationship between cyclone intensity with the extent of damage and forest recovery. The findings of our study indicate that the Polyhaline zone, the largest in terms of area and with the lowest elevation, suffered the most significant damage from cyclones in the Sundarbans region, likely due to its proximity to the most cyclone paths. A correlation analysis revealed that cyclone damage positively correlated with wind speed and negatively correlated with the distance of landfall from the center of the Sundarbans. With the expectation of more extreme weather events in the near future, the Sundarbans mangrove forest faces a potentially devastating outlook unless both natural protection processes and human interventions are undertaken to safeguard this critical ecosystem.

**Keywords:** Bay of Bengal; climate change; extreme weather events; natural hazards; NDVI; salinity zones; sea-level rise; tropical cyclone

## 1. Introduction

Mangrove forests, found along the coastal edges of many countries worldwide, cover an estimated 137,760–152,308 km<sup>2</sup> globally [1]. These ecosystems provide significant monetary value, contributing approximately \$1.6 billion annually to the global economy through various ecosystem services [2,3]. Beyond their economic importance, mangroves are highly

valued for their ecological benefits [4,5], particularly in protecting coastal areas from natural hazards and mitigating the effects of sea-level rise by keeping pace with erosion [6,7]. A recent study suggests that the global cyclone protection value of mangroves is worth about USD 1.8 million/km<sup>2</sup> per year [8]. However, despite their immense importance, mangrove ecosystems are declining worldwide due to various natural and human-induced threats including infrastructure development, aquaculture, and land conversion [9,10].

Tropical cyclones are significant natural disturbances that cause both short- and long-term changes in mangrove forests [11]. According to Sippo et al. [12], approximately 45% of reported mangrove disturbances and losses can be attributed to tropical cyclones. In addition, mangroves are more likely to be affected by tropical cyclones than other forests due to their location on the coast and exposure to higher wind energies during cyclones [13]. In mangrove ecosystems, in the short term, cyclones often lead to forest fragmentation and alterations in the landscape [12]. Over longer periods, these disturbances impact the succession, site productivity, and structural complexity of the forest [14]. Some countries like Bangladesh, Australia, and Myanmar are particularly vulnerable to cyclones, as they are frequently affected by tropical cyclones [11].

The Sundarbans in Bangladesh, the largest contiguous mangrove forest on Earth [15], face regular threats from sea-level rise, a consequence of global warming [16], and increasingly frequent and intense tropical cyclones over recent years [17]. By 2100, global sea levels are projected to rise by around 1 m or more [16], which is expected to impact the Sundarbans by altering the species composition of plants in different saline zones [18] and disrupting the natural habitats of various animal species [19].

Tropical cyclones originating in the Bay of Bengal continue to adversely affect the structure of the Sundarbans mangrove forest, despite a decrease in their overall number [17]. The damage caused by these cyclones, both short- and long-term, is making this unique ecosystem increasingly vulnerable to subsequent natural hazards. Therefore, it is crucial to analyze the damage from past cyclones to gain insights into the resilience of this ecosystem. Moreover, the Sundarbans is located at the estuary of the Ganges–Brahmaputra River, where salinity plays a vital role in shaping its ecosystem [20]. The forest is divided into three saline zones—Oligohaline (5–15 ppt), Mesohaline (15.1–25 ppt), and Polyhaline (>25 ppt)—based on soil salinity levels [21–23]. These zones significantly influence the spatial distribution of both flora and fauna within the mangrove forest [24]. Analyzing past and future disturbances across these zones is essential for understanding the resilience of this world-famous mangrove ecosystem.

Several studies have been conducted to assess disturbances in the Sundarbans mangrove forest, with a primary focus on cyclonic events [25–28]. Most of the research concentrates on the damage caused by one or more cyclones in Bangladesh and the Indian part of the Sundarbans [26,28–31]. Additionally, some studies have evaluated the Sundarbans' vulnerability to various other natural hazards [13,32–35]. Research involving the three saline zones of the Sundarbans has primarily focused on aspects such as tree diversity [18] and soil organic carbon [36]. However, studies specifically examining the vulnerability of these three saline zones in the Bangladesh Sundarbans to past cyclonic events are scarce. Such research is also crucial for identifying the most affected and vulnerable areas of the Sundarbans forest, guiding evidence-based future conservation efforts.

The present study investigates the impact of past major cyclonic disturbance events on the vegetation structure across three distinct saline zones in Bangladesh Sundarbans. The specific objective of the research is to determine the extent of vegetative areas disturbed by cyclones within each saline zone. The findings of this study will provide stakeholders with valuable insights into the distribution of cyclonic damage and the vulnerability of different saline zones, supporting the development of effective conservation plans and initiatives.

## 2. Materials and Methods

### 2.1. The Study Area

The Bangladesh Sundarbans cover approximately 6017 km<sup>2</sup>, making up 60% of the entire Sundarbans region [37]. This area is designated as a reserved forest and is man-

aged by the Bangladesh Forest Department (BFD). Geographically, it is situated in the world's second-largest watershed system—the lower Ganges–Brahmaputra delta [38]. The Sundarbans include three distinct wildlife sanctuaries: Sundarbans West WS (715 km<sup>2</sup>), Sundarbans South WS (370 km<sup>2</sup>), and Sundarbans East WS (310 km<sup>2</sup>). Additionally, it is recognized as a UNESCO World Heritage Site [39].

About 30% of the Sundarbans is interwoven with a complex network of rivers and streams of varying widths and depths [40]. The forest's elevation ranges from 0.5 m to 3.0 m above sea level, with 70% of the area lying below 1 m [19]. During regular tidal floods, much of the vegetation is submerged twice daily [41]. The soil in the region is finely textured, consisting primarily of silty clay loam [42].

The Bangladesh Sundarbans forest is divided into three zones based on soil salinity, i.e., Polyhaline, Mesohaline, and Oligohaline. The Oligohaline zone has low salinity (5–15 ppt), the Mesohaline zone has moderate salinity (15.1–25 ppt), and the Polyhaline zone is highly saline (>25 ppt) [21–23]. This mangrove forest represents a rich and diverse ecosystem, home to over 300 plant species and 1760 animal species including the famed Bengal tiger [15,43]. The predominant tree species include *Heritiera fomes*, *Excoecaria agallocha*, and *Ceriops decandra* and *E. agallocha* and *C. decandra* mainly in the Polyhaline zone [1]. Another climax species—*H. fomes*—is abundant in the Oligohaline zone [15].

## 2.2. Geospatial Analysis

### 2.2.1. Cyclone Dataset

The International Best Track Archive for Climate Stewardship (IBTrACS) dataset [44] was used to gather cyclone information. This study analyzed data from 12 cyclones (Figure 1) occurring between 2000 and 2020. From the IBTrACS dataset, we extracted and calculated the maximum sustained wind speed (km/h), landfall locations (within 500 km of the Bangladesh Sundarbans), cyclone paths, and the minimum distance (km) from the Sundarbans' center point (89.470445, 22.022068) (see Figure 1). Major cyclones of the last 25 years were investigated in the present study. The wind speed and the distance from the Sundarbans' central point of all the selected cyclones were gathered.

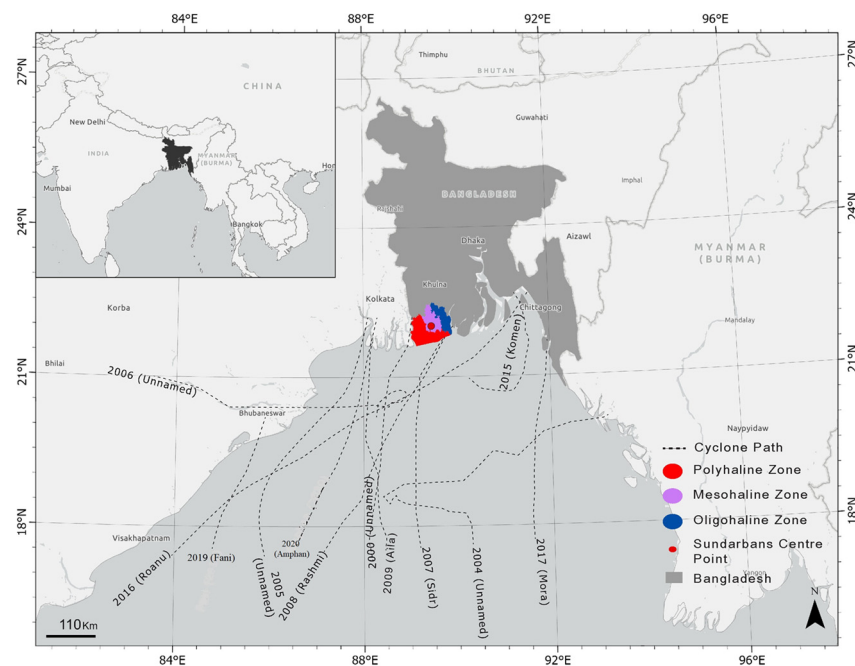


**Figure 1.** Path of the studied cyclones in the Bangladesh Sundarbans and the coverage of three saline zones (i.e., Polyhaline, Mesohaline, and Oligohaline) in the area. The red dot mark indicates the center point of the Sundarbans mangrove forest.

### 2.2.2. Earth Observation Dataset

For the analysis of cyclones from 2000 to 2020, surface reflectance datasets (Collection 2 Tier 1) from Landsat 5 and Landsat 8 were accessed via the Google Earth Engine (GEE) platform. The datasets used were identified by the image collection IDs LANDSAT/LT05/C02/T1\_L2 for Landsat 5 and LANDSAT/LC08/C02/T1\_L2 for Landsat 8. These surface reflectance datasets were atmospherically corrected using the LEDAPS (Landsat Ecosystem Disturbance Adaptive Processing System) for the Landsat 5 TM (Thematic Mapper) sensor [45] and LaSRC (Landsat 8 Surface Reflectance Code) for the Landsat 8 OLI (Operational Land Imager) sensor [46]. GEE automatically selected all images that intersected with the boundary of our study area.

### 2.2.3. Earth Observation Image Preprocessing

To assess the impact of cyclones, we followed the procedures outlined in Figure 2. To detect forest disturbances caused by cyclones and to evaluate recovery afterward, we calculated the Normalized Difference Vegetation Index (NDVI) [47] for two consecutive years: the year of the cyclone, representing the pre-cyclone NDVI, and the following year, representing the post-cyclone NDVI. Prior to data analysis, several preprocessing steps were performed to accurately measure the effects of cyclones. Cloud and cloud shadows were masked using the Quality Assessment (QA) band of the datasets. Additionally, a water mask was created using Global Hansen Data [48] to exclude water bodies from the study area images, ensuring that the NDVI analysis focused solely on vegetation, thereby yielding more accurate results [49].

To calculate pre- and post-cyclone NDVI, surface reflectance datasets were filtered according to specific date ranges for each cyclone (Table S1), creating image collections. These date ranges were chosen to produce image composites with minimal or no cloud cover and shadows [50]. The image collections were further filtered by cloud cover percentage, applying a threshold of 10%, except for cyclone Aila (40%) and Rashmi (50%), to generate cloudless composites for all cyclone analyses. The filtered image collections for pre- and post-cyclone periods were then reduced to a single image using the GEE function `ee.Reducer.median()`. These image composites represent pixel-wise median values from all images in the collection [50]. Consequently, two composites were produced for each cyclone, which were used to derive the pre- and post-cyclone NDVI. This approach has also been employed to analyze annual vegetation cover changes in the Sundarbans [29].

### 2.2.4. NDVI Classification

The pre- and post-cyclone NDVI images were calculated using the following equation:

$$\text{NDVI} = \frac{\rho_{\text{NIR}} - \rho_{\text{Red}}}{\rho_{\text{NIR}} + \rho_{\text{Red}}}$$

where  $\rho_{\text{NIR}}$  and  $\rho_{\text{Red}}$  represent near-infrared and red surface reflectance, respectively.

The pre- and post-cyclone NDVI images were each classified into four categories based on their NDVI values. Class 1, representing bare ground surfaces, included NDVI values ranging from 0 to 0.2 [51]. Class 2, with an NDVI range of 0.2 to 0.4, was assigned to areas with sparse or non-healthy vegetation, such as grass or shrubs. Class 3 and Class 4 corresponded to NDVI ranges of 0.4 to 0.6 and greater than 0.6, respectively, representing moderate and very dense vegetation. This NDVI classification follows the guidelines established by Kaplan and Avdan [52] and Idrees et al. [53].

To assess the impact of different cyclones, we compared the pre- and post-cyclone classified NDVI images, analyzing the transitions between NDVI classes after the cyclonic events using the `ee.Reducer.frequencyHistogram()` function in GEE. Forest gain was identified when areas transitioned from Class 1, Class 2, or Class 3 to Class 4, while forest loss was noted when areas moved in the opposite direction. For example, if a 10 km<sup>2</sup> area transitioned from Class 3 to Class 4, it was considered a forest gain. Conversely, a 15 km<sup>2</sup> area transitioning from Class 4 to Class 1 was considered a forest loss. This concept

was similarly applied to other class transitions to determine overall forest loss or gain. Additionally, analyses were conducted by saline zone to determine forest loss and gain in Polyhaline, Mesohaline, and Oligohaline zones.

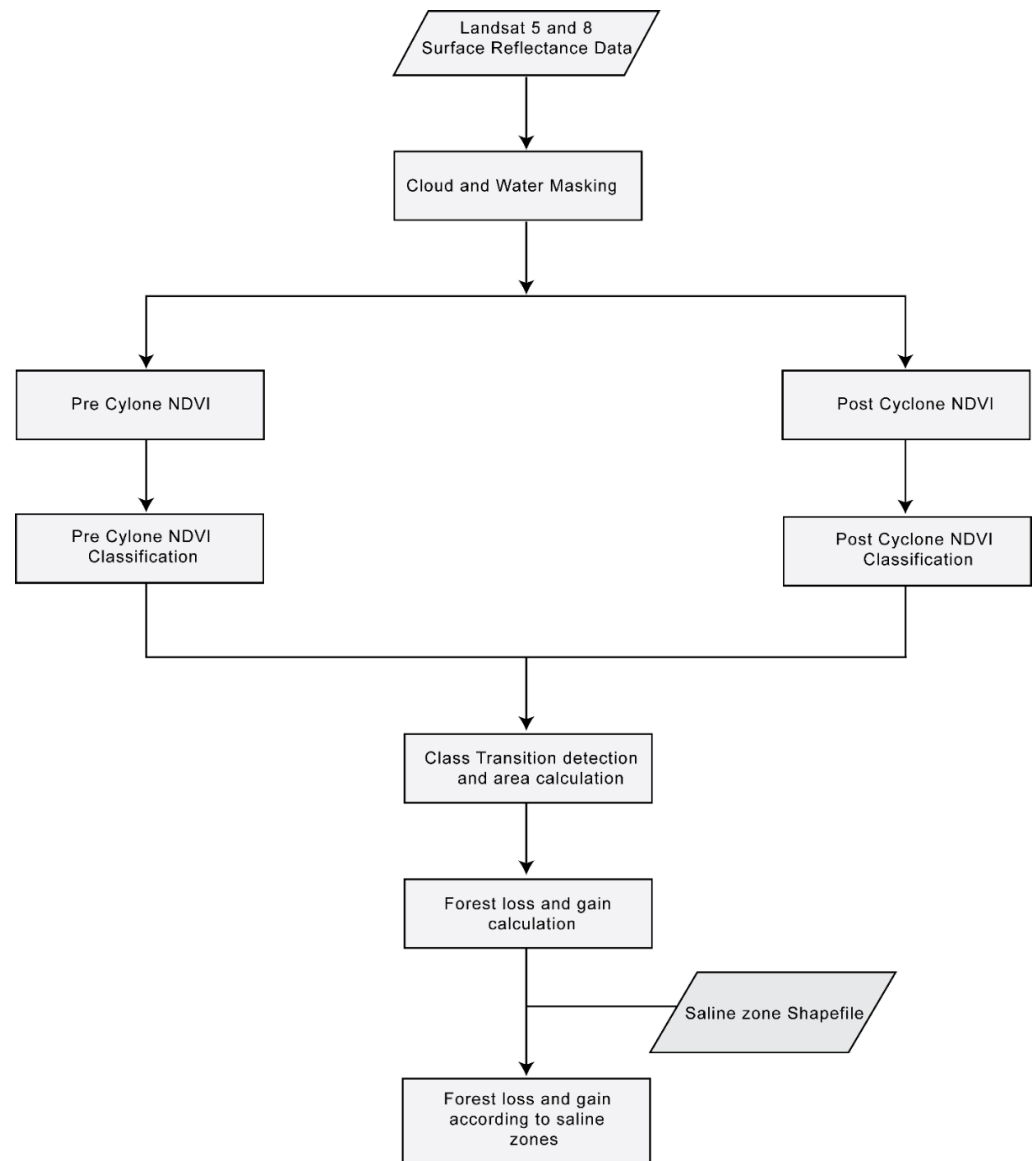


**Figure 2.** Flowchart of the working procedures of cyclone damage and recovery analysis.

### 2.3. Statistical Analysis

A one-way ANOVA was conducted to determine if there were significant differences in forest damage and recovery across the three saline zones. Tukey's HSD test was subsequently performed to identify the specific zones with significant differences. Prior to the ANOVA, the normality of the data for each saline zone was assessed using the Shapiro-Wilk test, and log transformation was applied as necessary to meet the assumptions.

We calculated the percentage of damaged area (damage%) and recovered area (recovered%) and analyzed the statistical relationship between damage% and other cyclone variables (wind speed and distance). Pearson's correlation, a non-parametric test, was used to measure these relationships after testing the assumptions of the correlation test, with log transformation applied where needed [54]. All statistical analyses were conducted using R software (version 4.4.0) [55]. For correlation analysis and visualization, the 'ggstatplot' and 'corrplot' packages were used [56,57].

### 3. Results

#### 3.1. Cyclones in the Sundarbans

##### 3.1.1. Class Transition of Mangrove Forest Vegetation

Due to distinct cyclone events, the Sundarbans forest in Bangladesh experienced significant shifts in various pre- and post-cyclone NDVI classes, which contributed to both forest loss and gain. Our results on class transitions indicate that all four NDVI classes underwent considerable changes after specific cyclones, with Sidr in 2007 being the most devastating (Figures 3 and 4; Table S2). Following the devastating Category 5 cyclone Sidr in 2007, only 2056.26 km<sup>2</sup> of the area (62.93 km<sup>2</sup> in Class 1, 85.08 km<sup>2</sup> in Class 2, 1641.96 km<sup>2</sup> in Class 3, and 266.29 km<sup>2</sup> in Class 4) remained unchanged, the lowest among all the cyclones studied, while 1999.89 sq. km were destroyed (Figures 3 and 4; Table S3). After Sidr 2007, the most significant NDVI transitions occurred following the Unnamed Cyclone of 2006, where the majority (1405.09 km<sup>2</sup>) of the transitions involved the conversion from pre-cyclone NDVI Class 4 to post-cyclone NDVI Class 3. In contrast, Cyclone Komen in 2015 had the least impact on the vegetation of the Sundarbans, with only minor transitions between NDVI classes and 3826.10 km<sup>2</sup> of the area remaining unchanged after the event (Figures 3 and 4; Table S2). The other nine cyclones showed varying degrees of NDVI class conversions.

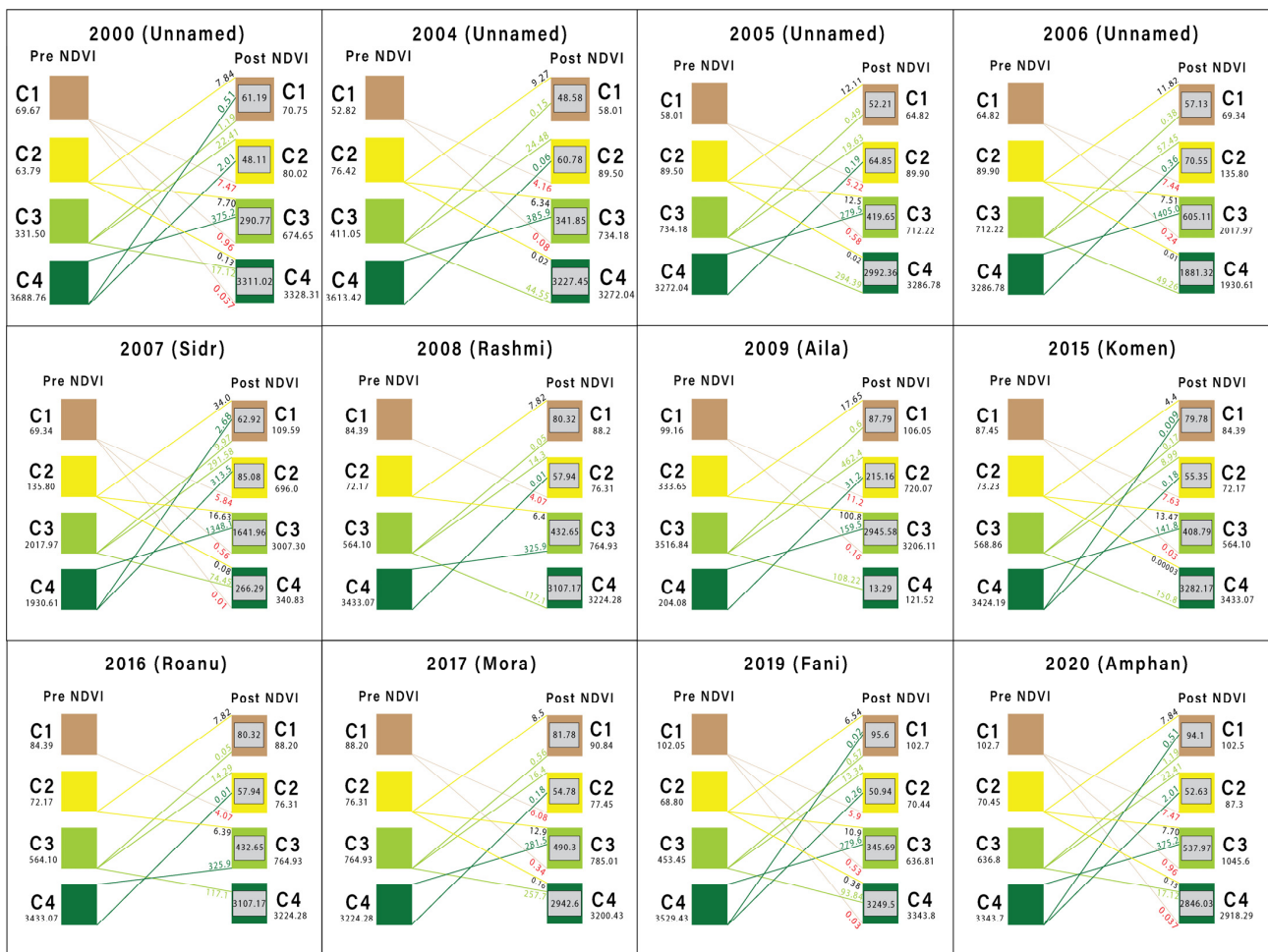


**Figure 3.** Transition of the four NDVI classes after the occurrence of cyclones and their transitioned amount in square kilometers (km<sup>2</sup>). C1, C2, C3, and C4 represent Class 1, Class 2, Class 3, and Class 4 of pre-cyclone and post-cyclone NDVI classes, respectively. The total amount of area (in km<sup>2</sup>) of each class of pre-cyclone and post-cyclone NDVI is given under the class identifier (C1, C2, C3, and C4). Gray-colored inset boxes represent the unchanged area of each NDVI class after cyclone occurrence. A distinct colored number at the end of each line illustrates the amount of area (in km<sup>2</sup>) shifted to other classes.

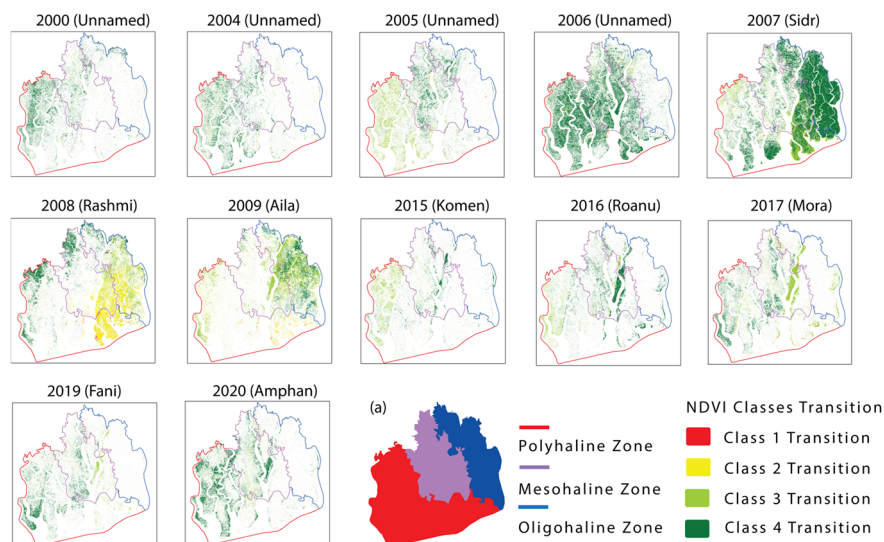


**Figure 4.** Transitioned area under different NDVI classes according to salinity zones in Bangladesh Sundarbans after the occurrence of 12 studied cyclones, where (a) represents the extent of the three saline zones.

### 3.1.2. Damaged Areas of Mangrove Forest Vegetation

Based on the measured NDVI class transitions, we calculated the loss and gain of forest coverage. Among the 12 cyclones analyzed in our study, only Cyclone 2007 (Sidr) caused significant damage, resulting in a 48.18% (1999.89 km<sup>2</sup>) loss of the forested area in the Sundarbans (Table 1; Figure 5). The unnamed cyclone of 2006 was the second most damaging, impacting 35.54% of the forest area (Table 1; Figure 5). Each of four other cyclones—2004 (Unnamed), 2008 (Rashmi), 2009 (Aila), and 2020 (Amphan)—led to more than a 10% reduction in vegetation cover in the Sundarbans mangrove forest in Bangladesh. In contrast, the remaining six cyclones—2000 (Unnamed), 2005 (Unnamed), 2015 (Komen), 2016 (Roanu), 2017 (Mora), and 2019 (Fani)—caused less than a 10% loss of vegetation (Table 1; Figure 5).

**Table 1.** Date of occurrence, distance from the center of Bangladesh Sundarbans, wind speed, damaged and recovered area for each studied cyclone.

Year (Cyclone Name)	Date	Distance (km)	Wind Speed (km/hour)	Damaged Area (km <sup>2</sup> )	Damage (%)	Recovered Area (km <sup>2</sup> )	Recovery (%)
2000 (Unnamed)	25–29 October	50.46	68.69	409.19	9.85	33.43	0.8055
2004 (Unnamed)	14–19 May	309	120	419.88	10.11	55.17	1.32
2005 (Unnamed)	1–3 October	110.12	142.14	311.93	7.51	312.72	7.53
2006 (Unnamed)	30 June–5 July	250	140	1475.11	35.54	64.49	1.55
2007 (Sidr)	10–16 November	44.4	259.28	1999.89	48.18	97.58	2.35
2008 (Rashmi)	24–27 October	38.4	83.34	415.24	10.005	647.63	15.60
2009 (Aila)	22–26 May	133.68	120.38	671.47	16.17	220.42	5.31
2015 (Komen)	26 July–2 August	100.28	74.28	155.61	3.74	172.02	4.14
2016 (Roanu)	17–22 May	117.095	115	348.06	8.38	127.57	3.073
2017 (Mora)	27–30 May	258.136	110	307.15	7.40	277.12	6.67
2019 (Fani)	25 April–4 May	150.6	200	300.36	7.23	111.64	2.69
2020 (Amphan)	16–21 May	121.51	220	532.21	12.82	90.78	2.18

A saline zone-wise analysis reveals that Cyclone 2009 (Aila) and Cyclone 2007 (Sidr) caused the most damage in the Oligohaline zone (Figures 5 and 6; Table S3). The Mesohaline zone experienced the most significant damage from Cyclone 2015 (Komen) and the unnamed cyclone of 2005 (Figures 5 and 6; Table S3). The remaining eight cyclones primarily affected the Polyhaline zone (Figures 5 and 6; Table S3).

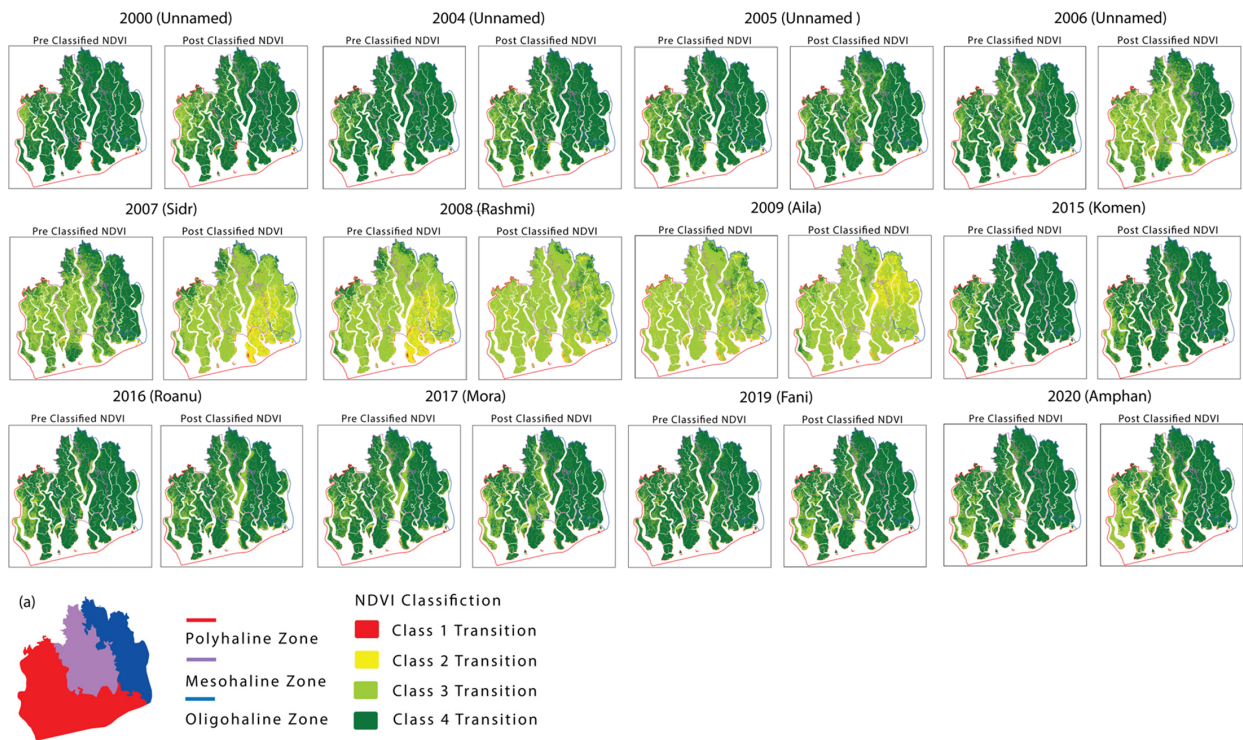


**Figure 5.** Four NDVI classes of both, pre-cyclone NDVI and post-cyclone NDVI, for the three saline zones of Bangladesh Sundarbans, where (a) represents the extent of the three saline zones.

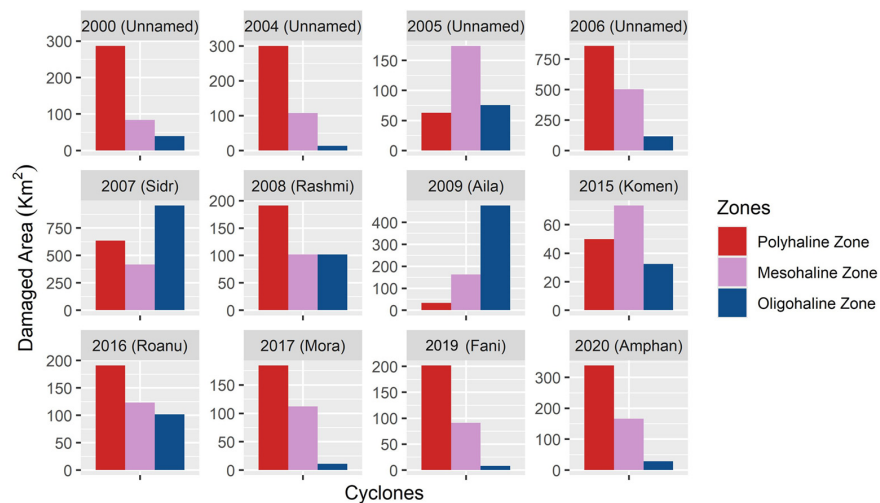


**Figure 6.** Cyclone-damaged areas in different saline zones are sorted by the year the cyclone occurred.

### 3.1.3. Recovery Areas of Mangrove Forest Vegetation

Despite the adverse impact of cyclones, some areas of the Sundarbans experienced natural vegetation recovery following these events. As shown in Figure 5 and Table 1, approximately 15.6% of the vegetation area recovered after Cyclone Rashmi in 2008, the highest recovery among all the cyclones studied. Cyclones 2005 (Unnamed), 2009 (Aila), and 2017 (Mora) also led to more than a 5% increase in vegetation cover (Table 1; Figure 3). In contrast, the remaining eight cyclones resulted in less than a 5% recovery of vegetation (Table 1; Figure 5).

Following Cyclones 2004 (Unnamed), 2005 (Unnamed), 2007 (Sidr), 2009 (Aila), and 2015 (Komen), the Polyhaline zone saw the most significant recovery (Figures 5 and 7; Table S3). Meanwhile, Cyclones 2006 (Unnamed), 2008 (Rashmi), and 2016 (Roanu) primarily triggered recovery in the Oligohaline zone (Figures 5 and 7; Table S3). The Mesohaline



zone experienced significant recovery after the remaining four cyclones: 2000 (Unnamed), 2017 (Mora), 2019 (Fani), and Amphan (2020 (Amphan) (Figures 5 and 7; Table S3).

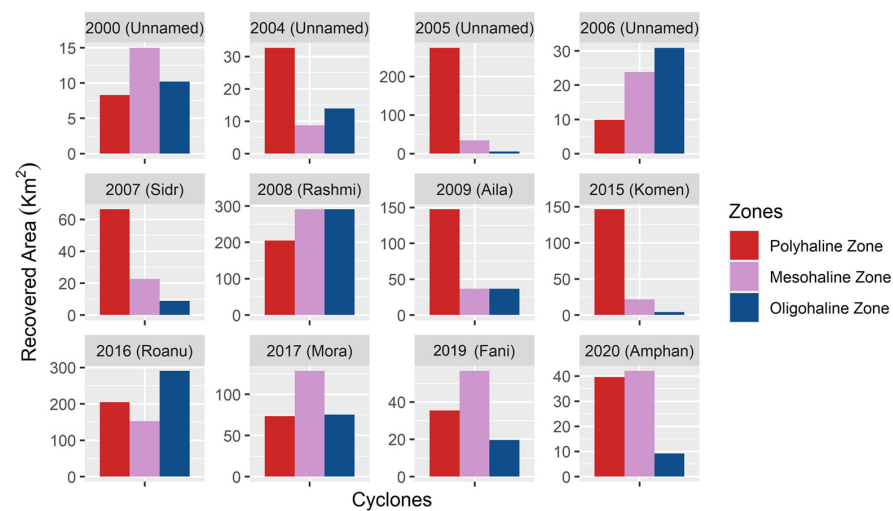


**Figure 7.** Cyclone-recovered areas in different saline zones sorted by the year of cyclone occurred.

### 3.2. Damage and Recovery of Mangrove Forest Vegetation in Three Saline Zones in Bangladesh Sundarbans

The results of our ANOVA analysis indicated that although the Polyhaline zone experienced greater damage compared to the other zones in Bangladesh Sundarbans, the difference was not statistically significant ( $p = 0.121$ ; Figure 8a). A similar trend was observed in the analysis of recovered areas, where no significant difference was found among the saline zones ( $p = 0.318$ ). However, the Polyhaline zone had the largest amount of recovered area compared to the other zones (Figure 8b).

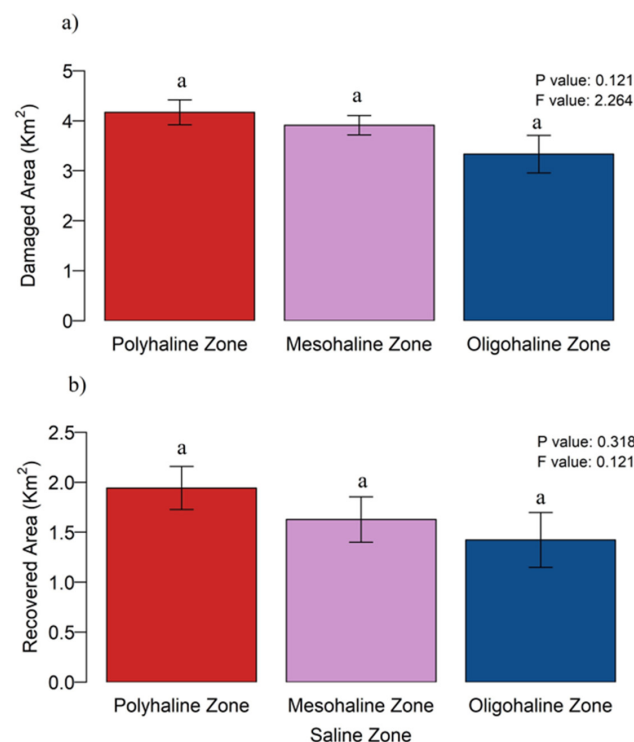


**Figure 8.** Mean saline zone-wise values of (a) the damaged area and (b) the recovered area. Here, similar letters were used to represent no significant difference among saline zone-wise damaged and recovered areas, respectively.

### 3.3. Correlation of Damage Percentage with Cyclone Variables

A correlation matrix was generated to examine the relationship between damage percentage and cyclone variables, specifically wind speed and distance (Figure 9a). Understanding this relationship helps identify which variable should be prioritized when predicting cyclone damage. Our results showed a positive correlation ( $r = 0.56$ ) between damage percentage and wind speed, although this relationship was not statistically significant ( $p > 0.05$ ) (Figure 9a,b). Similarly, a negative correlation ( $r = -0.01$ ) was found between damage percentage and distance, which was also not significant ( $p > 0.05$ ) (Figure 9a,c).

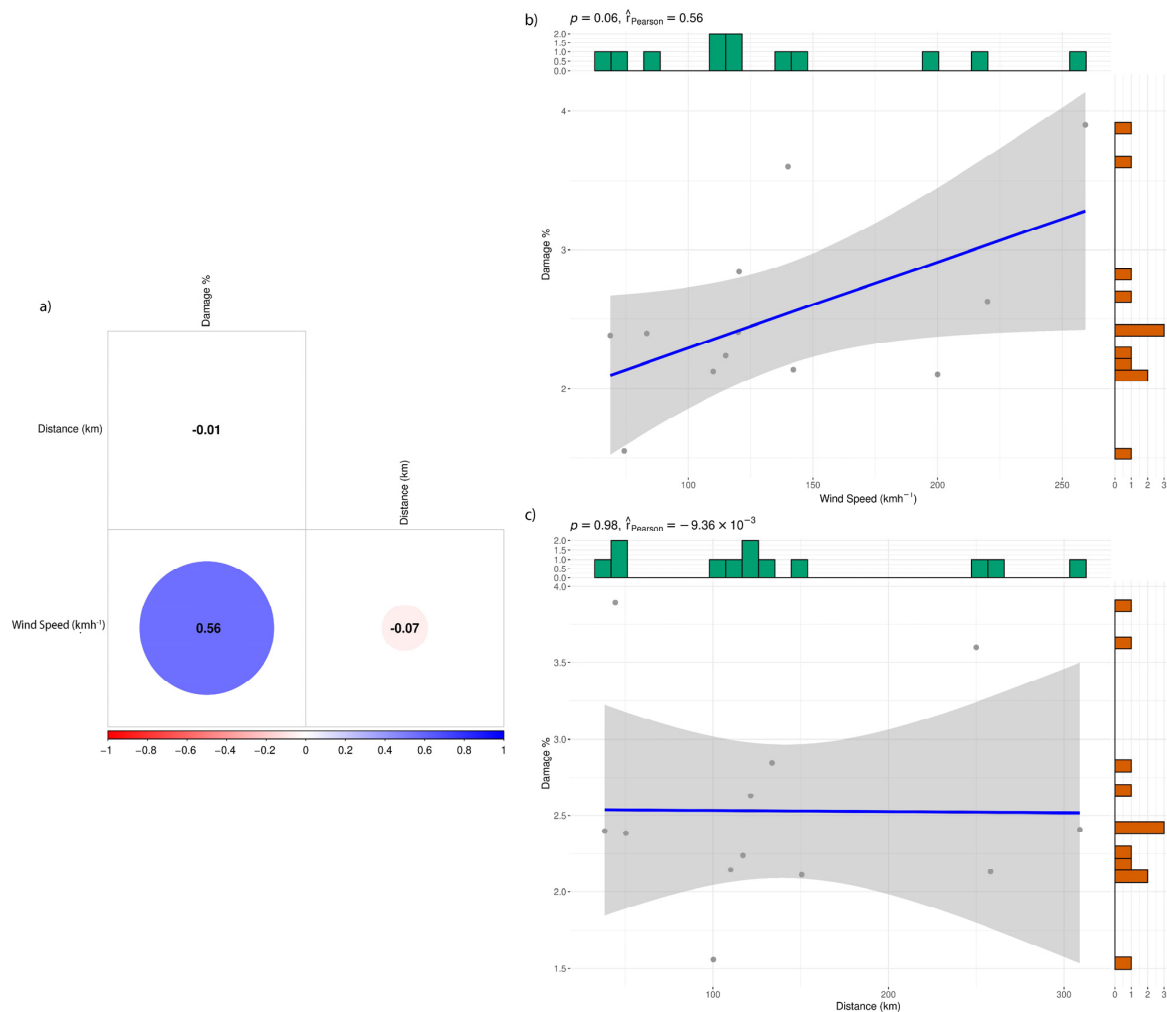


**Figure 9.** Results of correlation analysis of damage percentage (%) with cyclone variables, distance, and wind speed shown by (a) correlation matrix showing correlation coefficient values among different values; (b) results of Pearson's correlation among damage percentage and wind speed (c); results of Pearson's correlation among damage percentage and distance.

### 4. Discussion

Our 20-year cyclone analysis indicates that Cyclone 2007 (Sidr) has been the most devastating event in the Bangladesh Sundarbans mangrove forest (Table 1). This finding aligns with other multi-year cyclone hazard studies [11,17,26,35,58–61]. Hossain and Begum [62] further documented the devastation, reporting the loss of a single tree for every 100 m<sup>2</sup> due to the cyclone.

Our study estimated that approximately 48.18% of the area was damaged by Cyclone 2007 (Sidr), a figure higher than those reported in other studies [13,60,61]. Since our analysis considered class-wise transitions across four NDVI classes from 2000 to 2020, even the

destruction of the smallest vegetation patches (grass, shrub) was counted as forest damage. This comprehensive approach may have led to higher damage estimates compared to other studies.

Cyclones 2004 (Unnamed), 2008 (Rashmi), 2009 (Aila), and 2020 (Amphan) each accounted for about 10% of the damage to the Sundarbans mangrove forest in Bangladesh. Cyclone Amphan (2020), while particularly devastating to the Indian Sundarbans, where it affected a large portion of the forest (2400 km<sup>2</sup>), had a minimal impact on the Bangladeshi side of the Sundarbans [30,63]. Our findings indicate that Cyclone Aila caused significant damage across the entire Sundarbans forest, but most of its impact was concentrated in the Indian portion, with less damage observed in Bangladesh [26].

Rahman et al. [64] further highlighted the destruction caused by Cyclone 2009 (Aila), noting the uprooting and damage to several tree species, including Gewa (*E. agallocha*), and a significant decrease in the number of individual trees in the Sundarbans. Cyclone 2008 (Rashmi), a relatively weaker storm that occurred after Cyclone 2007 (Sidr), primarily caused vegetational damage through the transition from a very dense vegetation structure to a moderate vegetation class (Figure 3; Table S3), indicating its lower destructive capacity compared to other cyclones. Most of Cyclone Rashmi's damage was concentrated in the eastern part of the Sundarbans, where Dutta et al. [26] reported a 10% loss of vegetation.

Among the saline zones, the Polyhaline zone suffered the most significant damage from cyclones during the study period from 2000 to 2020 (Figures 5 and 6; Table S3). Eight out of the twelve cyclones studied caused severe damage to this zone compared to the Mesohaline and Oligohaline zones. The cyclone paths (Figure 1) were primarily directed toward the western part of the Sundarbans, making the Polyhaline zone particularly vulnerable to cyclone damage [13,65]. Additionally, the Polyhaline zone's large area and widespread distribution (Figure 1) make it the largest saline zone in the Bangladesh Sundarbans [21,66]. As a result, any cyclone impacting the Bangladeshi portion of the Sundarbans is likely to cause significant damage to the Polyhaline zone. The polyhaline zone is also situated in the southwestern, southern, and southeastern parts of the Bangladesh Sundarbans, regions that are particularly prone to cyclone damage originating from the North Indian Basin. Although our statistical analysis did not show a significant difference in vegetational damage across the saline zones, the Polyhaline zone still emerged as the most heavily damaged, followed by the Mesohaline and Oligohaline zones.

Cyclones 2007 (Sidr) and 2009 (Aila) were particularly devastating for the Bangladesh Sundarbans, especially for the Oligohaline zone, with 952.15 km<sup>2</sup> and 475.75 km<sup>2</sup> of this zone heavily damaged by these cyclones, respectively. The Mesohaline zone, on the other hand, experienced uniform damage throughout its extent from most of the cyclones studied. While there was no significant statistical difference in the vegetational damage values across the saline zones, the extent of damage varied by cyclone and zone.

The highest amount of recovery, at 15.6%, occurred after Cyclone 2008 (Rashmi), which is notable compared to the other 11 cyclones. As previously mentioned, Cyclone Rashmi was relatively weak [26,67] and did not cause significant vegetation damage or disrupt normal ecological processes. Consequently, the recovery process from the previous year's damage caused by Cyclone 2007 (Sidr) was not hindered, allowing for substantial vegetation regrowth.

Although the recovery in the Polyhaline zone was not significantly higher than in other zones, it remained the most prominent zone for recovery after most cyclones. The regeneration of a mangrove ecosystem after a catastrophic event depends on the availability of regeneration pathways, such as propagules or sprouting [68]. According to Harun-or-Rashid et al. [69], if a cyclone occurs near the fruiting season of mangrove species, the disturbed area can be quickly recolonized and regenerated by these species. In contrast, cyclones occurring outside the seeding season may favor the establishment of non-mangroves and mangrove associates, which are more tolerant to salinity and disturbances [70]. Additionally, disturbance- and saline-tolerant species like *E. agallocha*, which are fast-growing, can quickly occupy degraded regions [69].

Mangrove ecosystems have a remarkable ability to recover quickly [68,69,71], often beginning within one to six months after a disturbance, provided the necessary conditions are present in the ecosystem [68,69,72–74]. However, full recovery requires a much longer period [69,75,76].

Our results indicate a positive correlation between wind speed and vegetation damage. The force of cyclonic winds likely causes significant defoliation, uprooting, and litterfall [13,17,26], leading to negative changes in NDVI in the affected areas. This explains the positive relationship between wind speed and the extent of cyclone-induced damage. However, some studies suggest that mangrove forests can withstand cyclonic wind forces up to 101.86 km/h with minimal damage [13,26]. Beyond this threshold, wind force causes significant damage to all types of vegetation [77].

In our analysis, the minimum distance between the cyclone path and the center of the Sundarbans was a less influential factor. Nevertheless, major cyclones that made landfall in the Sundarbans have caused substantial damage [11,13]. Additionally, our data show that higher-magnitude cyclones, such as Cyclone Sidr (a Category 5 on the Saffir–Simpson Scale), were more destructive to the Bangladesh Sundarbans than Cyclone 2020 (Amphan), largely because Amphan's path was farther from the Bangladeshi portion of the Sundarbans compared to Sidr.

## 5. Conclusions

The Sundarbans mangrove forest in Bangladesh has long been a crucial defense for coastal areas and their inhabitants, shielding them from natural disasters while also serving as a vital source of income. This study found a positive correlation between wind speed, an indicator of cyclone intensity, and the damage caused by cyclones. This is particularly concerning for the Sundarbans, as recent reports indicate that while cyclone frequencies may decrease in future climate scenarios, their intensity is expected to increase significantly. The potential for more severe cyclones, combined with other natural hazards like sea-level rise, could place the Sundarbans Mangrove ecosystem in an ecologically precarious position.

One potential strategy to mitigate cyclone damage is the planting of wind-resistant trees to serve as coastal barriers in newly formed lands, degraded areas, and along the coastline. However, this study has several limitations that may have influenced the results. For instance, the impact of human disturbances was not considered in the analysis of NDVI changes in the study area. Additionally, using a more up-to-date distribution of saline zones could have yielded more accurate results. To better understand the regeneration process after cyclones, future research should consider analyzing a longer time span and using alternative vegetation indices, as NDVI has some limitations in assessing vegetation areas.

The findings of the present study will enhance our understanding of the potential impacts of cyclones, one of the most anticipated climate hazards in Bangladesh, on the Sundarbans mangrove forest ecosystem, particularly in relation to saline zones. This knowledge will be valuable in developing strategies to mitigate and minimize these effects. Additionally, the study's analysis of how each saline zone will be affected can help authorities prioritize and plan their interventions in alignment with the natural processes of ecosystems.

**Supplementary Materials:** The following supporting information can be downloaded at: <https://www.mdpi.com/article/10.3390/f15101722/s1>, Table S1: Date range and cloud cover percentage used in creating cloudless image composite for NDVI calculation of different cyclones; Table S2: Date of occurrence, distance from the center of Bangladesh Sundarbans, wind speed, damaged and recovered area for each cyclone; Table S3: Damaged and recovered area in different saline zones in sq. km unit.

**Author Contributions:** Conceptualization, M., F.S., S.K.S., S.A.M. and M.A.S.A.-K.; methodology, M., F.S., S.K.S., S.A.M. and M.A.S.A.-K.; software, M., A.K., S.A. and M.S.R.S.; validation, M. and M.S.B.; formal analysis, M. and F.S.; investigation, M. and F.S.; resources, M.A.S.A.-K.; data curation, M.; writing—original draft preparation, M., F.S., S.A.M. and M.A.S.A.-K.; writing—review and editing, A.K., S.A., M.S.R.S. and S.K.S.; visualization, M.; supervision, M.A.S.A.-K.; project administration,

M.A.S.A.-K.; funding acquisition, M., S.K.S., S.A.M. and M.A.S.A.-K. All authors have read and agreed to the published version of the manuscript.

**Funding:** We acknowledge the funding from the SUST Research Center (FES/2022/1/09, FES/2023/2/01) and the National Science and Technology Fellowship (NST, Session: 2021–22, Merit Serial: 92, Registration no: 55). This study also received partial support from the Asia-Pacific Network (APN) for Global Change Research (Japan) under the project “Protecting ecosystems and livelihoods of the Sundarbans, a World Heritage site: Assessing the impact of natural hazards on forest-based ecosystem services” (project code: CRRP2020-08MY-Srivastava), and the National Geographic Society (USA) under the project “Unlocking the potentials of Sundarbans mangrove forest as a nature-based climate solution” (grant reference number: NGS-78528R-22).

**Data Availability Statement:** The data presented in this study are available on request from the corresponding author.

**Acknowledgments:** We sincerely thank the faculty members of the Department of Forestry and Environmental Sciences at Shahjalal University of Science and Technology, Bangladesh, for their invaluable support. We are also grateful to our funding organizations, including the SUST Research Center (Bangladesh), the Asia-Pacific Network for Global Change Research (Japan), the National Geographic Society (USA), and the National Science and Technology Fellowship (Bangladesh).

**Conflicts of Interest:** The authors declare no conflicts of interest.

## References

- Giri, C.; Ochieng, E.; Tieszen, L.L.; Zhu, Z.; Singh, A.; Loveland, T.; Masek, J.; Duke, N. Status and distribution of mangrove forests of the world using earth observation satellite data. *Glob. Ecol. Biogeogr.* **2011**, *20*, 154–159. [[CrossRef](#)]
- Sarkar, P.; Banerjee, S.; Biswas, S.; Saha, S.; Pal, D.; Naskar, M.K.; Srivastava, S.K.; Barman, D.; Kar, G.; Mukul, S.A. Contribution of Mangrove Ecosystem Services to Local Livelihoods in the Indian Sundarbans. *Sustainability* **2024**, *16*, 6804. [[CrossRef](#)]
- Prusty, B.A.K.; Chandra, R.; Azeez, P.A. (Eds.) *Wetland Science*; Springer: New Delhi, India, 2017.
- Ismail, H.; Abd Wahab, A.K.; Alias, N.E. Determination of mangrove forest performance in reducing tsunami run-up using physical models. *Nat. Hazards* **2012**, *63*, 939–963. [[CrossRef](#)]
- Kathiresan, K. Importance of Mangrove Ecosystem. *Int. J. Mar. Sci.* **2012**, *2*, 70–79. [[CrossRef](#)]
- Krauss, K.W.; McKee, K.L.; Lovelock, C.E.; Cahoon, D.R.; Saintilan, N.; Reef, R.; Chen, L. How mangrove forests adjust to rising sea level. *New Phytol.* **2014**, *202*, 19–34. [[CrossRef](#)]
- Lovelock, C.E.; Cahoon, D.R.; Friess, D.A.; Guntenspergen, G.R.; Krauss, K.W.; Reef, R.; Rogers, K.; Saunders, M.L.; Sidik, F.; Swales, A.; et al. The vulnerability of Indo-Pacific mangrove forests to sea-level rise. *Nature* **2015**, *526*, 559–563. [[CrossRef](#)]
- Sun, F.; Carson, R.T. Coastal wetlands reduce property damage during tropical cyclones. *Proc. Natl. Acad. Sci. USA* **2020**, *117*, 5719–5725. [[CrossRef](#)] [[PubMed](#)]
- Mukul, S.A.; Huq, S.; Herbohn, J.; Seddon, N.; Lurance, W.F. Saving the Sundarbans from development. *Science* **2020**, *368*, 1198. [[CrossRef](#)]
- Polidoro, B.A.; Carpenter, K.E.; Collins, L.; Duke, N.C.; Ellison, A.M.; Ellison, J.C.; Farnsworth, E.J.; Fernando, E.S.; Kathiresan, K.; Koedam, N.E.; et al. The Loss of Species: Mangrove Extinction Risk and Geographic Areas of Global Concern. *PLoS ONE* **2010**, *5*, e10095. [[CrossRef](#)]
- Krauss, K.W.; Osland, M.J. Tropical cyclones and the organization of mangrove forests: A review. *Ann. Bot.* **2019**, *125*, 213–234. [[CrossRef](#)]
- Sippo, J.Z.; Lovelock, C.E.; Santos, I.R.; Sanders, C.J.; Maher, D.T. Mangrove mortality in a changing climate: An overview. *Estuar. Coast. Shelf Sci.* **2018**, *215*, 241–249. [[CrossRef](#)]
- Halder, N.K.; Merchant, A.; Misbahuzzaman, K.; Wagner, S.; Mukul, S.A. Why some trees are more vulnerable during catastrophic cyclone events in the Sundarbans mangrove forest of Bangladesh? *For. Ecol. Manag.* **2021**, *490*, 119117. [[CrossRef](#)]
- Simard, M.; Fatoyinbo, L.; Smetanka, C.; Rivera-Monroy, V.H.; Castañeda-Moya, E.; Thomas, N.; Van der Stocken, T. Mangrove canopy height globally related to precipitation, temperature and cyclone frequency. *Nat. Geosci.* **2019**, *12*, 40–45. [[CrossRef](#)]
- Aziz, A.; Paul, A. Bangladesh Sundarbans: Present Status of the Environment and Biota. *Diversity* **2015**, *7*, 242–269. [[CrossRef](#)]
- Payo, A.; Mukhopadhyay, A.; Hazra, S.; Ghosh, T.; Ghosh, S.; Brown, S.; Nicholls, R.J.; Bricheno, L.; Wolf, J.; Kay, S.; et al. Projected changes in area of the Sundarban mangrove forest in Bangladesh due to SLR by 2100. *Clim. Change* **2016**, *139*, 279–291. [[CrossRef](#)]
- Paul, B.K.; Rashid, H. Tropical Cyclones and Storm Surges. In *Climatic Hazards in Coastal Bangladesh*; Paul, B.K., Rashid, H., Eds.; Butterworth-Heinemann: Boston, MA, USA, 2017; pp. 35–81. [[CrossRef](#)]
- Sarker, S.K.; Matthiopoulos, J.; Mitchell, S.N.; Ahmed, Z.U.; Mamun, M.B.A.; Reeve, R. 1980s–2010s: The world’s largest mangrove ecosystem is becoming homogeneous. *Biol. Conserv.* **2019**, *236*, 79–91. [[CrossRef](#)]
- Mukul, S.A.; Alamgir, M.; Sohel, M.S.I.; Pert, P.L.; Herbohn, J.; Turton, S.M.; Khan, M.S.I.; Munim, S.A.; Reza, A.A.; Lurance, W.F. Combined effects of climate change and sea-level rise project dramatic habitat loss of the globally endangered Bengal tiger in the Bangladesh Sundarbans. *Sci. Total Environ.* **2019**, *663*, 830–840. [[CrossRef](#)]

20. Iftekhhar, M.S.; Saenger, P. Vegetation dynamics in the Bangladesh Sundarbans mangroves: A review of forest inventories. *Wetl. Ecol. Manag.* **2008**, *16*, 291–312. [[CrossRef](#)]
21. Hoque, M.A.; Sarkar, M.; Khan, S.; Moral, M.A.H.; Khurram, A.K.M. Present status of salinity rise in Sundarbans area and its effect on Sundari (*Heritiera fomes*) species. *Res. J. Agric. Biol. Sci.* **2006**, *2*, 115–121.
22. Rahman, M.M.; Khan, M.N.I.; Hoque, A.F.; Ahmed, I. Carbon stock in the Sundarbans mangrove forest: Spatial variations in vegetation types and salinity zones. *Wetl. Ecol. Manag.* **2015**, *23*, 269–283. [[CrossRef](#)]
23. Barik, J.; Mukhopadhyay, A.; Ghosh, T.; Mukhopadhyay, S.K.; Chowdhury, S.M.; Hazra, S. Mangrove species distribution and water salinity: An indicator species approach to Sundarban. *J. Coast. Conserv.* **2018**, *22*, 361–368. [[CrossRef](#)]
24. Ghosh, U.; Bose, S.; Brahmachari, R. *Sundarbans Living on the Edge: Climate Change and Uncertainty in the Indian Sundarbans*; STEPS Working Paper 101; STEPS Centre: Brighton, UK, 2018.
25. Bhowmik, A.K.; Cabral, P. Cyclone Sidr Impacts on the Sundarbans Floristic Diversity. *Earth Sci. Res.* **2013**, *2*, 2. [[CrossRef](#)]
26. Dutta, D.; Das, P.K.; Paul, S.; Sharma, J.R.; Dadhwal, V.K. Assessment of ecological disturbance in the mangrove forest of Sundarbans caused by cyclones using MODIS time-series data (2001–2011). *Nat. Hazards* **2015**, *79*, 775–790. [[CrossRef](#)]
27. Sakib, M.; Nihal, F.; Haque, A.; Rahman, M.; Ali, M. Sundarban as a Buffer against Storm Surge Flooding. *World J. Eng. Technol.* **2015**, *3*, 59–64. [[CrossRef](#)]
28. Akber, M.A.; Patwary, M.M.; Islam, M.A.; Rahman, M.R. Storm protection service of the Sundarbans mangrove forest, Bangladesh. *Nat. Hazards* **2018**, *94*, 405–418. [[CrossRef](#)]
29. Karsch, G.; Mukul, S.A.; Srivastava, S.K. Annual mangrove vegetation cover changes (2014–2020) in Indian Sundarbans National Park using Landsat-8 and Google Earth Engine. *Sustainability* **2023**, *15*, 5592. [[CrossRef](#)]
30. Mishra, M.; Acharyya, T.; Santos, C.A.G.; da Silva, R.M.; Kar, D.; Kamal, A.H.M.; Raulo, S. Geo-ecological impact assessment of severe cyclonic storm Amphan on Sundarban mangrove forest using geospatial technology. *Estuar. Coast. Shelf Sci.* **2021**, *260*, 107486. [[CrossRef](#)]
31. Hoque, M.A.-A.; Phinn, S.; Roelfsema, C.; Childs, I. Assessing tropical cyclone impacts using object-based moderate spatial resolution image analysis: A case study in Bangladesh. *Int. J. Remote Sens.* **2016**, *37*, 5320–5343. [[CrossRef](#)]
32. Akter, T.; Hoque, M.A.A.; Mukul, S.A.; Pradhan, B. Coastal Flood Induced Salinity Intrusion Risk Assessment Using a Spatial Multi-criteria Approach in the South-Western Bangladesh. *Earth Syst. Environ.* **2024**, 1–19. [[CrossRef](#)]
33. Sahana, M.; Hong, H.; Ahmed, R.; Patel, P.P.; Bhakat, P.; Sajjad, H. Assessing coastal island vulnerability in the Sundarban Biosphere Reserve, India, using geospatial technology. *Environ. Earth Sci.* **2019**, *78*, 304. [[CrossRef](#)]
34. Sahana, M.; Rehman, S.; Paul, A.K.; Sajjad, H. Assessing socio-economic vulnerability to climate change-induced disasters: Evidence from Sundarban Biosphere Reserve, India. *Geol. Ecol. Landsc.* **2021**, *5*, 40–52. [[CrossRef](#)]
35. Ali, S.A.; Khatun, R.; Ahmad, A.; Ahmad, S.N. Assessment of Cyclone Vulnerability, Hazard Evaluation and Mitigation Capacity for Analyzing Cyclone Risk using GIS Technique: A Study on Sundarban Biosphere Reserve, India. *Earth Syst. Environ.* **2020**, *4*, 71–92. [[CrossRef](#)]
36. Rahman, M.S.; Donoghue, D.N.M.; Bracken, L.J. Is soil organic carbon underestimated in the largest mangrove forest ecosystems? Evidence from the Bangladesh Sundarbans. *Catena* **2021**, *200*, 105159. [[CrossRef](#)]
37. Giri, C.; Pengra, B.; Zhu, Z.; Singh, A.; Tieszen, L.L. Monitoring mangrove forest dynamics of the Sundarbans in Bangladesh and India using multi-temporal satellite data from 1973 to 2000. *Estuar. Coast. Shelf Sci.* **2007**, *73*, 91–100. [[CrossRef](#)]
38. Rogers, K.G. Spatial and Temporal Sediment Distribution from River Mouth to Remote Depocenters in the Ganges-Brahmaputra delta, Bangladesh. Ph.D. Thesis, Vanderbilt University, Nashville, TN, USA, 2012.
39. Adyel, T.M.; Macreadie, P.I. World's Largest Mangrove Forest Becoming Plastic Cesspit. *Front. Mar. Sci.* **2021**, *8*, 766876. [[CrossRef](#)]
40. Islam, S.N.; Gnauck, A. Water salinity investigation in the Sundarbans rivers in Bangladesh. *Int. J. Water* **2011**, *6*, 74–91. [[CrossRef](#)]
41. Khan, M.A.R.; Dipu, S.; Ahmed, F. *Sundarban: Rediscovering Sundarban: The Mangrove Beauty of Bangladesh*; Nymphaea Publication: Dhaka, Bangladesh, 2013.
42. Choudhury, A.M. *Working Plan of the Sundarban Forest Division for the period 1960–61 to 1979–80*; East Pakistan Gov. Press: Dhaka, Bangladesh, 1968.
43. Ishtiaque, A.; Myint, S.W.; Wang, C. Examining the ecosystem health and sustainability of the world's largest mangrove forest using multi-temporal MODIS products. *Sci. Total Environ.* **2016**, *569–570*, 1241–1254. [[CrossRef](#)]
44. Knapp, K.R.; Kruk, M.C.; Levinson, D.H.; Diamond, H.J.; Neumann, C.J. The International Best Track Archive for Climate Stewardship (IBTrACS). *Bull. Am. Meteorol. Soc.* **2010**, *91*, 363–376. [[CrossRef](#)]
45. Masek, J.G.; Vermote, E.F.; Saleous, N.E.; Wolfe, R.; Hall, F.G.; Huemmrich, K.F.; Gao, F.; Kutler, J.; Lim, T.K. A Landsat Surface Reflectance Dataset for North America, 1990–2000. *IEEE Geosci. Remote Sens. Lett.* **2006**, *3*, 68–72. [[CrossRef](#)]
46. Vermote, E.; Justice, C.; Claverie, M.; Franch, B. Preliminary analysis of the performance of the Landsat 8/OLI land surface reflectance product. *Remote Sens. Environ.* **2016**, *185*, 46–56. [[CrossRef](#)]
47. Tucker, C.J. Red and photographic infrared linear combinations for monitoring vegetation. *Remote Sens. Environ.* **1979**, *8*, 127–150. [[CrossRef](#)]
48. Hansen, M.C.; Potapov, P.V.; Moore, R.; Hancher, M.; Turubanova, S.A.; Tyukavina, A.; Thau, D.; Stehman, S.V.; Goetz, S.J.; Loveland, T.R.; et al. High-Resolution Global Maps of 21st-Century Forest Cover Change. *Science* **2013**, *342*, 850–853. [[CrossRef](#)]

49. Mishra, K.; Prasad, P.R.C. Automatic Extraction of Water Bodies from Landsat Imagery Using Perceptron Model. *J. Comput. Environ. Sci.* **2015**, *2015*, 903465. [[CrossRef](#)]
50. Gorelick, N.; Hancher, M.; Dixon, M.; Ilyushchenko, S.; Thau, D.; Moore, R. Google Earth Engine: Planetary-scale geospatial analysis for everyone. *Remote Sens. Environ.* **2017**, *202*, 18–27. [[CrossRef](#)]
51. Aguilar, C.; Zinnert, J.C.; Polo, M.J.; Young, D.R. NDVI as an indicator for changes in water availability to woody vegetation. *Ecol. Indic.* **2012**, *23*, 290–300. [[CrossRef](#)]
52. Kaplan, G.; Avdan, U. Monthly Analysis of Wetlands Dynamics Using Remote Sensing Data. *ISPRS Int. J. Geo-Inf.* **2018**, *7*, 411. [[CrossRef](#)]
53. Idrees, M.O.; Omar, D.M.; Babalola, A.; Ahmadu, H.A.; Lawal, F.O. Urban land use land cover mapping in tropical savannah using Landsat-8 derived normalized difference vegetation index (NDVI) threshold. *S. Afr. J. Geomat.* **2022**, *11*, 117–129. [[CrossRef](#)]
54. Quinn, G.P.; Keough, M.J. *Experimental Design and Data Analysis for Biologists*; Cambridge University Press: Cambridge, UK, 2002.
55. R Core Team. R: A Language and Environment for Statistical Computing. 2017. Available online: <https://www.r-project.org/> (accessed on 5 January 2024).
56. Levy, M. Package ‘corrplot’. 2021. Available online: <https://cran.r-project.org/web/packages/corrplot/corrplot.pdf> (accessed on 5 January 2024).
57. Patil, I. Visualizations with statistical details: The “ggstatsplot” approach. *J. Open Source Softw.* **2021**, *6*, 3167. [[CrossRef](#)]
58. Scanes, C.G. Human Activity and Habitat Loss: Destruction, Fragmentation, and Degradation. In *Animals and Human Society*; Scanes, C.G., Toukhsati, S.R., Eds.; Academic Press: Cambridge, MA, USA, 2018; pp. 451–482.
59. Asher, S.; Garg, T.; Novosad, P. The Ecological Footprint of Transportation Infrastructure. Mimeo. 2017. Available online: [https://www.greenpolicyplatform.org/sites/default/files/downloads/resource/Asher\\_The%20Ecological%20Footprint%20of%20Transportation%20Infrastructure.pdf](https://www.greenpolicyplatform.org/sites/default/files/downloads/resource/Asher_The%20Ecological%20Footprint%20of%20Transportation%20Infrastructure.pdf) (accessed on 14 November 2023).
60. Cornforth, W.A.; Fatoyinbo, T.E.; Freemantle, T.P.; Pettorelli, N. Advanced land observing satellite phased array type L-Band SAR (ALOS PALSAR) to inform the conservation of mangroves: Sundarbans as a case study. *Remote Sens.* **2013**, *5*, 224–237. [[CrossRef](#)]
61. Ministry of Food and Disaster Management (MoFDM). *Super Cyclone Sidr 2007—Impacts and Strategies for Interventions*; MoFDM: Dhaka, Bangladesh, 2008; p. 75.
62. Hossain, M.; Begum, M. Vegetation of Sunderban Mangrove Forest after the Devastating Cyclone Sidr in Bangladesh. *Soc. Change* **2011**, *5*, 72–78.
63. Islam, M.T.; Charlesworth, M.; Aurangojeb, M.; Hemstock, S.; Sikder, S.K.; Hassan, M.S.; Dev, P.K.; Hossain, M.Z. Revisiting disaster preparedness in coastal communities since 1970s in Bangladesh with an emphasis on the case of tropical cyclone Amphan in May 2020. *Int. J. Disaster Risk Reduct.* **2021**, *58*, 102175. [[CrossRef](#)]
64. Rahman, S.; Rahman, H.; Shahid, S.; Khan, R.U.; Jahan, N.; Ahmed, Z.U.; Khanum, R.; Ahmed, M.F.; Mohsenipour, M. The impact of Cyclone Aila on the Sundarban forest ecosystem. *Int. J. Ecol. Dev.* **2017**, *32*, 88–97.
65. Mita, K.S.; Azad, A.A.; Zaman, M.W.; Sakib, M.; Amin, G.M.R.; Asik, T.Z.; Haque, A.; Rahman, M.M. Effectiveness of Adaptive Measures against Storm Surge Hazard. based on Field Experience from a Real. Time Cyclone in Bangladesh Coast. In Proceedings of the Poster presented in the Collaborative Adaptation Research Initiative in Africa and Asia, Dhaka, Bangladesh, 24 October 2018.
66. Deb, J.C.; Rahman, H.M.T.; Roy, A. Freshwater Swamp Forest Trees of Bangladesh Face Extinction Risk from Climate Change. *Wetlands* **2016**, *36*, 323–334. [[CrossRef](#)]
67. Mandal, M.S.H.; Hosaka, T. Assessing cyclone disturbances (1988–2016) in the Sundarbans mangrove forests using Landsat and Google Earth Engine. *Nat. Hazards* **2020**, *102*, 133–150. [[CrossRef](#)]
68. Aung, T.T.; Mochida, Y.; Than, M.M. Prediction of recovery pathways of cyclone-disturbed mangroves in the mega delta of Myanmar. *For. Ecol. Manage* **2013**, *293*, 103–113. [[CrossRef](#)]
69. Harun-or-Rashid, S.; Biswas, S.R.; Böcker, R.; Kruse, M. Mangrove community recovery potential after catastrophic disturbances in Bangladesh. *For. Ecol. Manage* **2009**, *257*, 923–930. [[CrossRef](#)]
70. Wang, L.; Mu, M.; Li, X.; Lin, P.; Wang, W. Differentiation between true mangroves and mangrove associates based on leaf traits and salt contents. *J. Plant Ecol.* **2011**, *4*, 292–301. [[CrossRef](#)]
71. Leal, M.; Spalding, M.D. (Eds.) *The State of the World’s Mangroves*; Global Mangrove Alliance: Washington, DC, USA, 2024. [[CrossRef](#)]
72. Hu, T.; Smith, R. The Impact of Hurricane Maria on the Vegetation of Dominica and Puerto Rico Using Multispectral Remote Sensing. *Remote Sens.* **2018**, *10*, 827. [[CrossRef](#)]
73. Primavera, J.H.; Dela Cruz, M.; Montilijao, C.; Consunji, H.; Dela Paz, M.; Rollon, R.N.; Maranan, K.; Samson, M.S.; Blanco, A. Preliminary assessment of post-Haiyan mangrove damage and short-term recovery in Eastern Samar, central Philippines. *Mar. Pollut. Bull.* **2016**, *109*, 744–750. [[CrossRef](#)]
74. Taylor, M.D.M.R.B.; Rangel-Salazar, J.L.; Hernández, B.C. Resilience in a Mexican Pacific Mangrove after Hurricanes: Implications for Conservation Restoration. *J. Environ. Prot. (Irvine. Calif.)* **2013**, *4*, 1383–1391. [[CrossRef](#)]
75. Imbert, D. Hurricane disturbance and forest dynamics in east Caribbean mangroves. *Ecosphere* **2018**, *9*, e02231. [[CrossRef](#)]

- 
76. Macamo, C.C.F.; Massuanganhe, E.; Nicolau, D.K.; Bandeira, S.O.; Adams, J.B. Mangrove's response to cyclone Eline (2000): What is happening 14 years later. *Aquat. Bot.* **2016**, *134*, 10–17. [[CrossRef](#)]
  77. Sarker, M.M.H.; Gain, A.K.; Paul, N.K.; Biswas, S.R. A trait-based approach to quantify ecosystem services delivery potentials in the Sundarbans mangrove forest of Bangladesh. *Ecol. Indic.* **2024**, *166*, 112390. [[CrossRef](#)]

**Disclaimer/Publisher's Note:** The statements, opinions and data contained in all publications are solely those of the individual author(s) and contributor(s) and not of MDPI and/or the editor(s). MDPI and/or the editor(s) disclaim responsibility for any injury to people or property resulting from any ideas, methods, instructions or products referred to in the content.